Stretching and Scaling in Polymeric Micelles

Kathleen A. Cogan† and Alice P. Gast*

Department of Chemical Engineering, Stanford University, Stanford, California 94305-5025

Malcolm Capel

Biology Department, Brookhaven National Laboratory, Building 463, Upton, New York 11973

Received May 7, 1991; Revised Manuscript Received August 7, 1991

ABSTRACT: We probe the details of block copolymer micelle structure with small-angle X-ray and neutron scattering. Working with polystyrene/poly(ethylene oxide) diblock copolymers in cyclopentane and deuterated cyclohexane, we can control micelle aggregation numbers by adding trace amounts of water[1,2] and can therefore modulate the deformation of the polystyrene blocks in the micelle coronae. We compare our measurements with predictions of a starlike model that assumes semidilute conditions throughout the micelle corona. Scaling behavior consistent with the model is observed for micelles with large polystyrene blocks at Θ conditions. The signature scattering of a random coil in the intermediate scattering region begins at a larger scattering vector for the polystyrene blocks constrained to the micelle coronae compared to that for an unperturbed coil. The semidilute solution in the micelle coronae is characterized by a z-average blob size that decreases with increasing aggregation number. Scattering in the intermediate region from micelles of smaller, more symmetric copolymer indicates the polystyrene blocks are stretched so severely that they do not undergo a random walk on any length scale. These results illustrate the strong interplay between copolymer composition and micelle structure.

Introduction

In recent years there has been increasing interest in the configurations of polymers in constrained geometries,[3] from adsorbed block copolymers and end-grafted chains at planar interfaces to the spherical geometries of multiarmed star polymers and block copolymer micelles. Often the high local concentration in these structures leads to highly stretched chain trajectories, quite different from the random-walk configurations of an isolated chain. In amphiphilic systems the concentration profiles are determined from a free energy balance of enthalpic and entropic contributions. Micellization is driven by the phase separation of insoluble blocks into microscopic domains whose size is limited in part by deformation of the soluble blocks. The extent of the deformation varies with copolymer composition; more symmetric copolymers tend to form micelles with higher aggregation numbers containing chains with more severely perturbed configurations. A uniform core–shell model[4-9] has provided a useful first approximation to describe micelle structure despite the unrealistic assumption of a constant concentration profile in the micelle corona. Recent theoretical[10-14] and experimental studies[15-17] of concentration profiles in star molecules offer an improved picture of chain configurations in constrained spherical geometries. In particular, we have applied the scaling model of Daoud and Cotton[10] to develop a starlike micelle model, with a uniform core of insoluble blocks surrounded by a semidilute solution of soluble blocks.[18]

We initially applied this model to interpret dynamic and static light scattering measurements of large poly(ethylene oxide)/polystyrene (PEO/PS) block copolymer micelles in cyclopentane.[2] Due to the compatibility of PEO and water, we can change the number of chains in these micelles by a factor of 4 by adding trace amounts of water and forming micelles with cores of PEO and water. In the previous study, we have found the radius of gyration and hydrodynamic size of micelles with aggregation numbers on the order of 80 are well described by the starlike model. In this paper we use the manipulation of micelle size by addition of water as a method for altering the density profiles of the constrained blocks in the micelle coronae.

Complete scattering profiles from these micellar solutions should contain features of both dilute and semidilute solutions, as found in studies of star molecules.[17,19] Scattering at small scattering vectors provides information about the overall size of an isolated micelle, as in the light scattering study described above. The larger scattering vectors in small-angle X-ray and neutron scattering experiments probe length scales within the micelles. In particular, these measurements should provide a more direct test of the validity of the starlike micelle model to describe the coronal chain density profiles. In the pioneering SAXS study of block copolymer micelles by Plestil and Baldrian,[4] the signal at intermediate scattering vectors was attributed to scattering from the micellar cores. Alternatively, Picot and co-workers have associated the scaling exponents in this regime with local chain configurations.[20,21] In this paper we consider scattering from a semidilute solution in the micelle corona in addition to that of the core in the interpretation of scattering in the intermediate region.

We begin by presenting a summary of the starlike micelle model, followed by a description of the small-angle X-ray (SAXS) and neutron (SANS) experiments. We first consider SAXS measurements of dilute polystyrene solutions in order to discuss scattering from unperturbed coils. Here we also test the physical parameters used later to predict polystyrene concentration profiles in the micelle coronae. We then present results for the large asymmetric block copolymers investigating the dependence of micelle structure on aggregation number. Finally, we study micelles of relatively short symmetric block copolymers. These micelles illustrate the profound influence of geometrical constraints on the structure of polymer chains and point out the limitations of a scaling model for the description of concentration profiles for short

† Present address: Cygnus Therapeutic Systems, 400 Penobscot Drive, Redwood City, CA 94063.

0024-9297/91/2224-6512$02.50/0

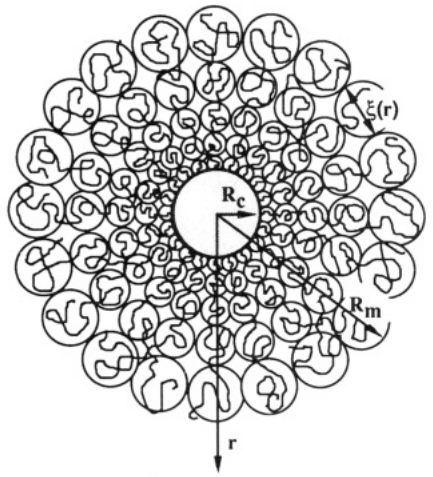

Figure 1. Schematic of a starlike micelle. R_c, R_m, and $\xi(r)$ denote the core radius, micelle radius, and diameter of a blob, respectively.

chains in highly constrained geometries.

Starlike Micelle Model

We expand on the model proposed by Daoud and Cotton describing the radial concentration profile in a star polymer.[10] We envision a micelle comprising a homogeneous core of insoluble blocks and dispersed solvent surrounded by a semidilute solution of soluble blocks, as illustrated in Figure 1. A complete description of the model is presented in previous publications.[2,18]

Each block in the micelle corona can be modeled as a string of blobs with increasing blob size at longer radial distances. Since one end of each block emanates from the surface of the micelle core, the highest polymer concentration and smallest blob size are found near the micelle core. Smaller blobs are found in micelles containing more chains. The exact relationship between blob size, ξ, aggregation number, f, and radial distance, r, results from requiring that the cross-sectional area of f blobs at a distance r match the surface area of a sphere with radius r, yielding $\xi(r) = 4r/\sqrt{f}$.

We predict the polymer volume fraction profile in the micelle corona by considering the polymer concentration within each blob. By definition, there are $(\xi/a_s)^{1/\nu}$ monomers/blob, where the Flory swelling exponent, ν, is $^1/_2$ at Θ conditions and a_s is the statistical segment length. We determine the radius of the core, R_c, and the entire micelle, R_m, for a particular aggregation number by integrating over the density profile and conserving mass. Our final result is a volume fraction profile weighted by the contrast between each component and the solvent

$$n(r) = \begin{cases} (n_c - n_o) & r < R_c \\ (n_s - n_o) A V_s (r/a_s)^{1/\nu} r^{-3} & R_c < r < R_m \\ 0 & R_m < r \end{cases} \quad (1)$$

with $A = 3(4^{1/\nu}) f^{(3\nu-1)/2\nu}/32\pi$ and V_s denoting the volume of a statistical segment. The contrast of the core, n_c, is a volume fraction average of the contrasts for the insoluble block and any dispersed solvent. Differences in indexes of refraction determine the contrast in light scattering experiments, whereas X-ray and neutron scattering measurements depend on differences in electron densities, ρ^X, and scattering length densities, ρ^N. Note that the model does not contain any adjustable parameters.

We can predict several length scales characterizing micelle structure as a function of aggregation number. In the derivation of the profile, we have assessed the core and overall size of the micelle. The micelle radius of gyration is obtained from the second moment of the volume fraction profile. Small-angle scattering measurements probing length scales within the micelle can further test the validity of the model for describing micelle structure. When appropriate, we can then calculate an average blob size for the chains in the micelle corona to compare with an average correlation length measured with small-angle X-ray or neutron scattering.

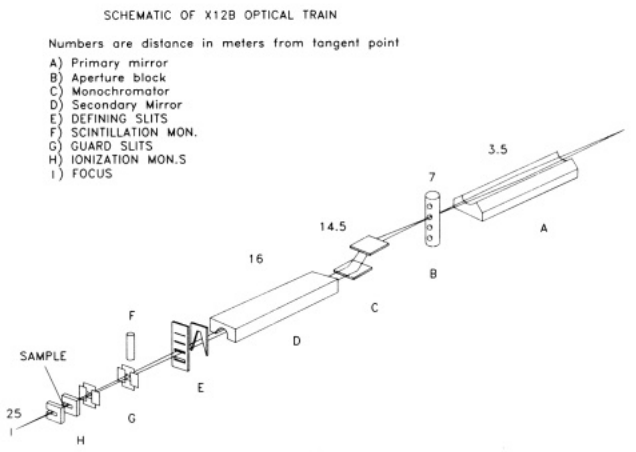

Figure 2. Schematic of the optical train at NSLS experimental station X12B.

Table I
SAXS from Dilute Solutions of Polystyrene Homopolymer

PS	$M_w \times 10^{-3}$ [a]	$M_w \times 10^{-3}$ [b]	M_w/M_n [a]	R_g, [b] nm	R_g, [c] nm
1540	160	146	1.10	11.8	10.6
590	61	57	1.03	6.9	6.6
85	9	8	1.04	2.2	2.5

[a] Values cited by Polysciences, Inc. [b] Averages measured from Zimm and Guinier plots. [c] Predictions from the Kuhn model (see text).

Experimental Section

1. Materials. We purchased polystyrene–poly(ethylene oxide) diblock copolymers SE002 and SE003 from Polymer Laboratories, Inc. They report molecular weights of 187 500 and 11 140 with corresponding ethylene oxide contents of 4 and 25.5 wt %, determined from gel permeation chromatography (GPC) measurements of the polystyrene block and NMR experiments on the final block copolymer. Polydispersity indexes, M_w/M_n, equal to 1.10 and 1.12 are assessed from GPC measurements of the block copolymer. The samples will be identified by listing the degrees of polymerization of the two blocks, i.e., PEO/PS = 170/1730 and PEO/PS = 65/80.

Three polystyrene standards whose properties are listed in Table I were purchased from Polysciences, Inc. Cyclopentane purchased from Eastman Kodak with a purity of 99% was used in the X-ray scattering samples. Solvent purification performed in initial studies[1] has been deemed unnecessary. Deuterated (99.7%) cyclohexane for the neutron scattering experiments was purchased from Cambridge Isotope Laboratories. Block copolymer and homopolymer solutions were studied at concentrations of 0.75–1.5 wt %.

2. Small-Angle X-ray Scattering. We collected all of the SAXS data presented here at the National Synchrotron Light Source (NSLS) Station X12B, dedicated to time-resolved small-angle diffraction (TRSAD). The facility consists of three principal components: the optical train; the spectrometer (including sample handling systems); and the data acquisition system.

Figure 2 is a diagram of the optical train of the TRSAD facility. The first optical element is a mirror of a toroidal figure, whose function is to focus white radiation onto a circular slit array 7 m from the bending magnet servicing the beamline. Downstream of a Be window, radiation passes through a pair of flat Si 111

Table II
Electron Densities ρ^X and Scattering Length Densities ρ^N

segment	ρ, g cm^{-3}	ρ^X, Å^{-3}	$\rho^N \times 10^{-10}$,[d] cm^{-2}
polystyrene	1.06[a]	0.343	1.42
poly(ethylene oxide)	1.13[a]	0.371	0.64
cyclopentane	0.742[b]	0.255	
deuterated cyclohexane	0.909[c]		6.84
water	1.0	0.334	−0.56

[a] From ref 22. [b] At 23 °C from ref 23. [c] From ref 25. [d] Calculated from coherent scattering lengths in ref 26.

crystals (fixed exit geometry), providing monochromatic radiation of wavelength between 0.7 and 1.7 Å (band-pass of order 10^{-4}). The monochromatic radiation is refocused by a bent-cylindrical mirror to a point approximately 0.3 × 0.3 mm (25 m from the bending magnet). Beam conditioning is accomplished by defining slits and two guard slit arrays. The brilliance on the sample at a wavelength of 1.38 Å is approximately 10^{11} photons/s/0.1% band-pass.

The TRSAD spectrometer has mechanisms to align the sample and X-ray beam. Detectors can be positioned anywhere from 50 to 330 cm from the sample position. The spectrometer also allows the detectors to be rotated about the sample (−15° to +60°). In these experiments up to 20 samples were sequenced into the beam with a Rigaku reflectance diffractometry sample changer modified to operate in transmission geometry. X-ray flux is continuously monitored immediately upstream and downstream of the sample with a pair of miniature ionization counters. Sample cells have a nominal path length of 1.6 mm, 55 μL volume, defined by Kapton windows. Because of the low surface tension and volatility of cyclopentane, we used Torr Seal low pressure resin to attach the Kapton windows to the Kel-F sample cells. The sample ports were sealed by compressing small pieces of lightly cross-linked Viton, generously provided by Equal Elastomers of Ohio, providing minimal sample loss for periods greater than 1 month.

A custom-built (BNL Instrumentation Division) high-speed one-dimensional delay line gas detector was used to collect data. This detector has an active area of 10 × 2 cm (slitted down to ca. 2 mm off axis, digitized to provide 950 channels, maximum count rate 10^5 events/s). Digitized data are routed to either a pulse height analyzer (Tracor Norther, TN-1750) or a time-slicing data acquisition system (BNL Instrumentation Division).

All X-ray scattering measurements were performed on cyclopentane solutions at 23 °C, where polystyrene is near Θ conditions.[2] Calculated electron densities listed in Table II reveal that all micelle components have similar contrast relative to cyclopentane. Data were acquired in sets of 5 min, for a total of 30–180 min. Sample to detector distances ranged from 63 to 206 cm, providing scattering vectors $0.007 \text{ Å}^{-1} < q < 0.35 \text{ Å}^{-1}$ calibrated from diffraction peaks of collagen and cholesteryl myristate. Scattering profiles were corrected for thickness and transmission before the solvent scattering was subtracted.[24] Intensities are most sensitive to subtraction errors at high scattering vectors. Scattering profiles in this region were verified by utilizing the diffraction peaks originating from a Kapton window on the vacuum tube between the sample and the detector. The amount of solvent scattering subtracted was determined by minimizing the appearance of the Kapton peak located at an arbitrary, large scattering vector. Absolute intensities for the measurements of the polystyrene standards were obtained from comparison with the scattering from a Lupolen standard.[24]

Preliminary measurements of these micellar solutions were performed on beamline I-4 at the Stanford Synchrotron Radiation Laboratory (SSRL).

3. Small-Angle Neutron Scattering. Small-angle neutron scattering experiments were performed at the Institut Laue-Langevin (ILL). Measurements were taken with sample to detector distances of 1.4 m at D17 and 3.2 m at D11, covering scattering vectors $0.008 \text{ Å}^{-1} < q < 0.3 \text{ Å}^{-1}$ with a neutron wavelength of 10.2 Å and 10% monochromatization. All experiments were done at 40 °C where polystyrene in deuterated cyclohexane is near Θ conditions.[25] Solvent scattering and an estimate of incoherent scattering from the dissolved polymer were subtracted from the scattering profiles before normalizing the intensity scale to a water standard. Micelle molecular weights were obtained by comparison with a 0.8 wt % solution of the PS = 590 standard listed in Table I. The contrast for the micelle was estimated by a volume fraction average of the component scattering length densities listed in Table II.

4. Dynamic Light Scattering. We use a Brookhaven Instruments BI-200 goniometer equipped with a Lexel Model 95 2-W argon ion laser to measure the hydrodynamic sizes of our micelles. Digital signals from the goniometer are processed using a Brookhaven Instruments BI2030 136-channel correlator. We invert the temporal correlation functions with the data analysis program CONTIN,[27] developed by Provencher. CONTIN determines the smoothest nonnegative hydrodynamic size distribution that is consistent with the data. In order to reduce possible distortions due to oversmoothing, we decrease the weighting of the curvature penalty term by setting the "probability one to reject" to 0.2, less smoothing than suggested by Provencher. We then compare several data sets (on the order of ten) at each angle to assess the reliability of the resultant distributions. Details of the data analysis are discussed in a recent publication.[1]

Results and Discussion

Polystyrene Solutions. We first consider small-angle X-ray scattering measurements from dilute solutions of polystyrene homopolymer. These scattering profiles provide a reference for comparison with measurements of our micellar solutions. Scattering from dilute polymer solutions comprises three regions.[28] Information on smaller length scales is obtained at larger angles; the length scale is inversely proportional to the scattering vector, $q = (4\pi/\lambda) \sin(\theta/2)$, where λ is the radiation wavelength and θ is the angle between the incident and detected X-rays. The overall shape of the polymer coil dominates the intensity at small scattering vectors. The radius of gyration is commonly measured from the angular dependence of the intensity at small scattering vectors using either the Guinier approximation

$$I(q) = I(0)\, e^{-q^2 R_g^2/3} \tag{2}$$

or the Zimm approximation

$$\frac{1}{I(q)} = \frac{1}{I(0)}\left[1 + \frac{q^2 R_g^2}{3}\right] \tag{3}$$

Kirste et al.[29] have shown that a combination of the Zimm and Guinier methods is preferred over isolated use of either in the analysis of polymer coils. This is recommended even in the range encompassing $qR_g = 1$ since the radius of gyration is overestimated in the Zimm method and underestimated in the Guinier analysis. Average values from both methods are listed in Table I for three polystyrene standards. Alternatively, Ullman[30] has calculated correction factors for the Zimm analysis that depend on the polydispersity and the range of scattering vectors used in the fit. We find results similar to those listed in Table I using this methodology.

We compare the measured radii of gyration with predictions from Kuhn's model for freely jointed chains[31] in Table I. Since we study cyclopentane solutions at 23 °C, near the Θ temperature, we expect the chains to follow Gaussian statistics. We define the statistical segment length as $a_s^2 = 6R_g^2/N_s$ and determine from the data of Berry[32] that polystyrene in cyclohexane at Θ conditions has $a_s = 1.55$ nm, equivalent to 5 monomers/statistical segment. Assuming similar chain configurations at Θ conditions in cyclopentane and cyclohexane, we use the number of statistical units, N_s, determined from the measured molecular weights to predict R_g and find agreement to within 13%.

Small-angle neutron scattering experiments[33] have shown that the configurations of low molecular weight

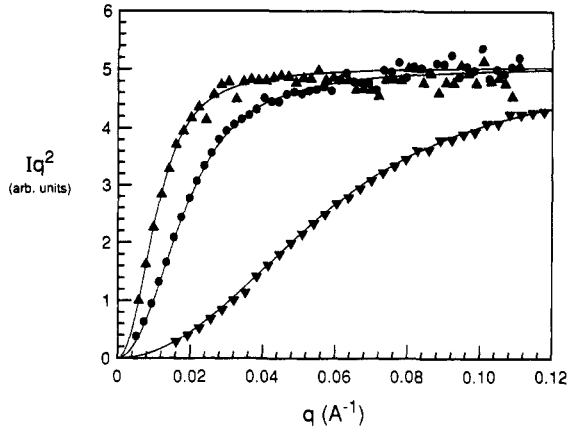

Figure 3. Kratky plots from SAXS of dilute polystyrene solutions in cyclopentane, with (▲) 1.30 wt % PS = 1540, (●) 1.60 wt % PS = 590, and (▼) 1.26 wt % PS = 85. Solid lines represent the Debye equation using the measured radii of gyration listed in Table I. The intermediate scattering region is observed for the two largest molecular weights.

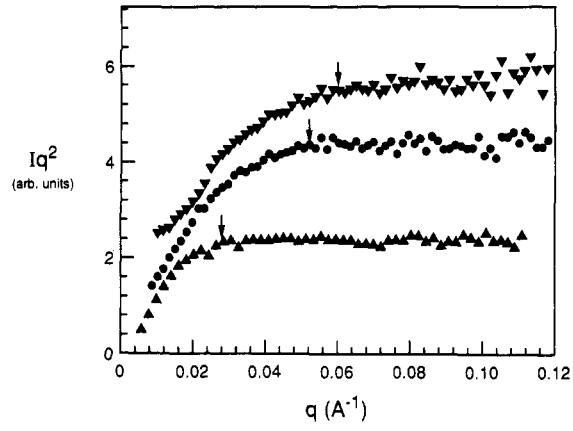

Figure 4. Kratky plots from SAXS of PEO/PS = 170/1730 micelles and PS = 1540 chains. Micellar solutions are (▼) 1.01 wt % copolymer saturated with water and (●) 0.87 wt % copolymer with 30 ppm water, whereas the polystyrene solution (▲) is 1.30 wt % polymer. Minimum scattering vectors for scaling behavior, q^*, are indicated by arrows. Single-chain correlations are first observed at larger scattering vectors for the perturbed polystyrene chains constrained to the micelle coronae.

polystyrene in deuterated cyclohexane at Θ conditions are well described by the wormlike chain model of Porod and Kratky with a persistence length of 0.88 nm. Since the persistence length corresponds to half of the Kuhn statistical length, this value agrees well with the statistical length cited above. The Kuhn model overestimates the radius of gyration if there are not enough statistical units to obey Gaussian statistics. For a solution of 4000 molecular weight polystyrene, R_g is 12% lower than the Kuhn estimate.[33] We find a similar deviation in R_g for our polystyrene standard with a molecular weight of 9000, indicating that this sample is near the minimum molecular weight needed to follow Gaussian statistics.

In the intermediate scattering region, it is possible to resolve details of the chain configurations. Debye's equation[34] for scattering from isolated random coils

$$I(q) = I(0)\left(\frac{2}{x^2}\right)(x - 1 + e^{-x}) \qquad (4)$$

where $x = q^2R_g^2$, predicts that the intensity should scale as q^{-2} in the limit of large scattering vectors. More generally, the scaling exponent of −2 corresponds to $-1/\nu$, where the Flory swelling exponent ν is $^1/_2$ for chains at Θ conditions. A third region is found at larger scattering vectors where one is probing individual segments and the chain appears as a collection of needles. The scattering is expected to scale as q^{-1} at scattering vectors larger than $3.82/a_s$,[35] corresponding to a scattering vector of 0.25 Å^{-1} for polystyrene chains at Θ conditions.

The Kratky plots in Figure 3 clearly illustrate the regions where we observe the intensity scaling for the polystyrene standards; i.e., a plateau represents the expected exponent of −2. We also show that Debye's equation, based on the radii of gyration we measured at low scattering vectors, provides good descriptions of the entire scattering profiles for all three polymers. The largest measured scattering vectors are well within the intermediate region for the PS = 1540 and PS = 590 samples. Note that, as expected, the minimum q for the scaling behavior decreases with increasing molecular weight, illustrating that correlations between monomers are evident at longer length scales for larger chains. The intermediate scattering region is not observed for the PS = 85 standard. Debye's relationship suggests intensity scaling as q^{-2} will begin at scattering vectors larger than 0.15 Å^{-1}.

Yoon and Flory have employed rotational isomeric state theory to describe the configurational characteristics of polystyrene.[36] Scattering profiles have been generated by treating the substituted carbon atom in each styrene repeat unit as a point scatterer. The resulting intensities decay more slowly than q^{-2} in the intermediate scattering region, deviating from both the experimental profiles of the dilute homopolymer solutions in Figure 3 and the expected behavior from Debye's equation. In the present study we focus on perturbations to chain configurations as they are constrained to the dense structure of copolymer micelles; we interpret our results by making direct comparisons between our micellar solution scattering profiles and those measured from dilute homopolymer solutions.

Micellar Solutions of Asymmetric Copolymer. We have shown that structures formed in cyclopentane solutions of polystyrene/poly(ethylene oxide) diblock copolymers are very sensitive to trace amounts of water.[1,2] The addition of water lowers the effective critical micelle concentration, equivalent to lower concentrations of single chains in solutions with more water. In fact, using dynamic light scattering we can barely detect any single chains in solutions saturated with water. Karl Fischer titrations of saturated solutions reveal that the micelle cores contain 0.7 molecule of water/ethylene oxide repeat unit.[1] Solutions with higher concentrations of water contain micelles with higher aggregation numbers and, hence, more severely perturbed chain configurations. Here we focus our attention on small-angle X-ray scattering measurements of solutions of the PEO/PS = 170/1730 copolymer; earlier studies discuss static[2] and dynamic[1,2] light scattering measurements. As we increase the water content from 30 ppm to saturation levels with copolymer concentrations on the order of $\sim 10^{-3}$ g/mL, the hydrodynamic radius increases from 35 to 44 nm and the number of chains per micelle grows from 17 to 77. We use this ability to manipulate association to investigate the validity of the starlike model, considering a combination of the dynamic light scattering and the static light and X-ray scattering measurements.

We probe the details of micelle structure with small-angle X-ray scattering and expect to find scattering characteristics of semidilute solutions if the starlike model is valid. This is illustrated in Figure 4 where we show Kratky plots for PEO/PS = 170/1730 block copolymer solutions both saturated and with 30 ppm water in addition

to a solution of the PS = 1540 standard. All three curves exhibit intermediate scattering regions indicative of chains undergoing a random walk. The fact that the intensity decays as q^{-2} does not, however, demonstrate that a semidilute solution is attained in the micelle coronae. This behavior would be expected whether the chains in the micelle corona were primarily in contact with each other or had large portions dangling as isolated chains in solution. More pertinent is the value of the minimum scattering vector, q^*, of the intermediate region.

The characteristic decay in the intermediate scattering region can be derived by considering the pair correlation function for a random coil, $g(r) \propto 1/r$, in the limit of short distances.[37] The intensity scaling behavior ($\propto q^{-2}$) follows from taking the Fourier transform of the pair correlation function. At higher concentrations where the coils overlap, interactions between monomers are screened by the close proximity of other chains and the pair correlation function decays more rapidly. The length scale where monomers become uncorrelated is characterized by the blob size or screening length. In these semidilute solutions, the signature scattering of the intermediate region is found at smaller length scales, i.e., at scattering vectors large enough to probe within the blobs.

It is significant then to compare q^* for the data presented in Figure 4. Correlations within a single chain are evident at significantly longer length scales (smaller q^*) for the polystyrene homopolymer, PS = 1540, than for the PEO/PS = 170/1730 block copolymer micelles. Since the homopolymer is roughly the same size as the soluble block in the micelles, the 2-fold difference in q^* demonstrates that the blocks in the micelle coronae are substantially perturbed when constrained to the coronal geometry. It is also interesting to compare the end-to-end distance of the PS = 1540 chains, 20 nm, and the distance traversed by a polystyrene block in the micelle corona, $R_h - R_c$, 32 and 38 nm, for micelles with 17 and 77 chains, respectively.

Other, more subtle differences are evident in the scattering curves from the two micellar solutions. The top curve in Figure 4 corresponds to micelles saturated with water, with an aggregation number 4 times that of the unsaturated micelles. The larger q^* indicates slightly smaller blob sizes in the micelles containing more chains. Furthermore, the scattering profile differs at low scattering vectors, where the change in curvature may indicate the tail of a maximum in the Kratky plot. A maximum would represent an enhancement of the radial segment distribution function compared to that for a random coil,[38] and its magnitude should increase for micelles containing more chains. A maximum is observed for the smaller micelles described below.

A number of investigators[39-41] have measured the screening length, ξ_E, in semidilute solutions using the relationship originally proposed by Edwards.[42]

$$I(q) \propto \frac{1}{1 + q^2\xi_E^2} \tag{5}$$

Measurement of the screening length is similar to determination of R_g from a Zimm plot. The PEO/PS = 170/1730 copolymer data in Figure 5 display ξ_E of 6.2 and 5.1 nm for micelles with aggregation numbers of 17 and 77, respectively. The smaller screening length characterizing the interior of micelles with more chains is indicative of a higher local polymer concentration.

We compare the measured screening lengths with predictions from the starlike micelle model based on aggregation numbers measured from light scattering. We expect to measure an average screening length in our micellar solutions since the polymer concentration is not uniform in the micelle coronae. Analogous to the z-average square radius of gyration measured from a polydisperse collection of coils,[43] we propose that at intermediate scattering vectors a Zimm plot for starlike structures should yield a z-average square radius of gyration of the blobs in the micelle corona, $R_{g,blob}^2 = \xi^2/6$ and the micelle core, $R_{g,core}^2 = (3/5)R_c^2$. Whereas the light scattering average is weighted by the square of the polymer mass and refractive index increment, $\langle R_g^2\rangle_z = \sum\{M^2(\partial n/\partial c)^2 R_g^2\}/\sum\{M^2(\partial n/\partial c)^2\}$, the z-average in X-ray scattering is weighted by the square of the polymer volume and the difference in electron densities, $\langle R_g^2\rangle_z = \sum\{V^2(\rho^X - \rho_o^X)^2 R_g^2\}/\sum\{V^2(\rho^X - \rho_o^X)^2\}$. Recalling the radial dependence of the blob size, $\xi^2 = 16r^2/f$, and the polymer volume fraction profile given in eq 1, we integrate over ξ^2 in the micelle corona and obtain

$$\langle R_g^2\rangle_{z,b+c} = \frac{\frac{128}{3f^{3/2}a_s^4}V_s^2(\rho_s^X - \rho_o^X)^2(R_m^6 - R_c^6) + \frac{16}{15}\pi^2(\rho_c^X - \rho_o^X)^2 R_c^8}{\frac{24}{f^{1/2}a_s^4}V_s^2(\rho_s^X - \rho_o^X)^2(R_m^4 - R_c^4) + \frac{16}{9}\pi^2(\rho_c^X - \rho_o^X)^2 R_c^6} \tag{6}$$

We present a summary of predicted and measured values in Table III; the measured $\langle R_g^2\rangle_{z,b+c}$ equals $3\langle \xi_E^2\rangle_z$. The average blob size is clearly dominated by the large blobs at the outer edges of the corona even though the concen-

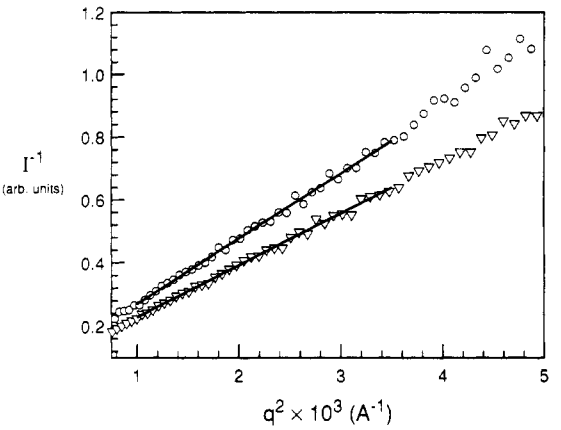

Figure 5. Determination of the average blob size in the PEO/PS = 170/1730 micellar solutions, where ▽ denotes a 1.01 wt % copolymer solution saturated with water and ○ a 0.87 wt % copolymer solution with 30 ppm water. Similar q ranges have been used to measure screening lengths in semidilute solutions of polystyrene.[40,41] The smaller blob size in the micelles saturated with water demonstrates stronger perturbations of coronal chains in micelles with higher aggregation numbers.

Table III
PEO/PS = 170/1730 Micelle Characteristics

	Light Scattering	
aggregation no.	17	77
	Starlike Micelle Model	
R_c, nm	3.5	6.4
R_m, nm	34.0	49.7
$\xi(R_c)$, nm	3.4	2.9
$\xi(R_m)$, nm	33.0	22.7
$\langle\xi^2\rangle_{z,blob}^{1/2}$, nm	26.9	18.5
$R_{g,core}$, nm	2.7	5.0
$\langle R_g^2\rangle_{z,blob}^{1/2}$, nm	11.0	7.6
$\langle R_g^2\rangle_{z,b+c}^{1/2}$, nm	10.8	6.4
	Small-Angle X-ray Scattering	
$\langle\xi_E^2\rangle_z^{1/2}$, nm	6.2	5.1
$\langle R_g^2\rangle_{z,b+c}^{1/2}$, nm	10.7	8.8

tration of polymer and, hence, contrast is smallest for these blobs. The micelle cores account for 0.4% and 29% of the predicted $\langle R_g^2 \rangle_{z,b+c}$ in the micelles with 17 and 77 chains, respectively. The core contribution becomes more significant in micelles with more chains because, in addition to the larger core volume, the coronae contain smaller blobs.

In our previous light scattering study,[2] we found good agreement between the measured and theoretical radii of gyration for micelles saturated with water. Corresponding hydrodynamic sizes 3–4 nm smaller than the overall radius predicted from the starlike model indicate a small amount of draining in the outer edges of the micelles. The radius of gyration prediction for micelles at low water content (aggregation number = 17) falls below the measured value. Similarly, molecular dynamics simulations of star polymers display deviations from the scaling model for stars with fewer than 20 arms.[11] When there are too few chains in a micelle, the arms in the corona are not stretched into the string of blobs supposed in the star model. Note that since the blob size increases continuously in the radial direction, $\xi(r)$ represents both the distance between neighboring arms and the tangential distance occupied by monomers within one arm. The model predicts a blob size at the outer edge of the 17 chain micelle, 33.0 nm, larger than the thickness of the corona, $R_m - R_c$ = 30.5 nm. Thus the chains do not overlap with neighboring chains at the outer edges of these micelles. It is clear that semidilute conditions exist throughout the corona of a micelle with 77 chains; here the maximum blob size, 22.7 nm, is significantly smaller than both the corona thickness, 43.3 nm, and the end-to-end distance, 29 nm, of a polystyrene arm if it was not constrained in the micelle corona.

The starlike model forces each block copolymer to occupy a wedge. If the blocks are not at semidilute concentrations throughout the corona, it will overestimate the blob size at the outer edge of the micelle while underestimating the micelle radius of gyration. Neutron scattering of six-armed polystyrene stars with labels at the outer edges of the arms displays a smaller screening length than anticipated,[44] suggesting that the arms do not overlap at the edges of the six-armed stars. Our X-ray scattering measurement of the average blob and core radius of gyration $\langle R_g^2 \rangle_{z,b+c}^{1/2}$ = 10.7 nm for the micelles with 17 chains is very close to the predicted value. Hence, this result implies that 17 is close to the minimum number of chains necessary for micelle structure to be described by the starlike micelle model. However, it may be difficult to distinguish through the average blob size measurement between micelles with coronal chain ends dangling like random coils or slightly perturbed by other chains. These two cases should be more discernible via comparison of the predicted and measured micelle radii of gyration. In particular, for small numbers of arms, f, there is a crossover between $\langle R_g^2 \rangle$ scaling as Nf for f = 1 and 2 to $Nf^{1/2}$ for many arms, illustrating that, for a given molecular weight, a star polymer with many arms will be much more compact than a structure similar to a random coil. Indeed, the ratio of gyration to hydrodynamic radii clearly illustrates structural changes as a function of aggregation number.[2]

The average blob size is smaller in micelles with more chains, although the measured change in $\langle R_g^2 \rangle_{z,b+c}^{1/2}$ from 10.7 to 8.8 nm is less dramatic than the predicted change from 10.8 to 6.4 nm. The large polystyrene concentration near the core–corona interface may provide an explanation for the larger discrepancy in values for the micelles with 77 chains. The small blobs near the core contain fewer than 10 statistical units, too few to expect a random walk on a local scale. We predict $\langle R_g^2 \rangle_{z,b+c}^{1/2}$ = 8.8 nm if we extend the solid core radius to include the portion of the polystyrene corona contained in blobs with 11 statistical units or less, treating the rest of the polystyrene in the corona as a semidilute solution with a decreasing concentration profile. Despite the complications in interpretation of the measured average radius of gyration of a blob, it is clear that the polystyrene blocks are more strongly deformed in the corona of the micelles with more chains. The change in the predicted average blob size corresponds to a polystyrene concentration increase from 2.9 to 4.2% by volume as the aggregation number increases from 17 to 77.

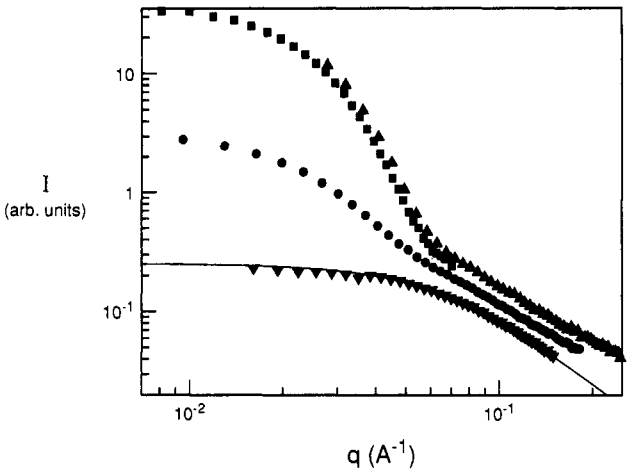

Figure 6. Scattering profiles from (▼) SAXS of a 1.26 wt % solution of PS = 85 homopolymer, (●) SAXS of a 1.25 wt % cyclopentane solution of PEO/PS = 65/80 micelles saturated with water, (■ and ▲) SANS of a 0.99 wt % deuterated cyclohexane solution of PEO/PS = 65/80 micelles saturated with water. The solid line represents Debye's equation for the scattering profile from a dilute solution of PS = 85 homopolymer. Although the SAXS data for the micelles and homopolymer are arbitrarily scaled for clarification and the SANS and SAXS data are similarly scaled, the two sets of SANS data, ■ and ▲, are normalized on the scattering of water.[48]

Micellar Solutions of Symmetric Copolymer. Solutions of the symmetric copolymer, PEO/PS = 65/80, exhibit sensitivity to the presence of water similar to that described above. Samples with relatively small amounts of water contain nonspherical aggregates in addition to single chains and spherical micelles.[1] Higher concentrations of water are needed to dissipate the PEO/PS = 65/80 aggregates because of the larger fraction of poly(ethylene oxide) in this sample. Above 100 ppm of water, a 0.5 wt % copolymer solution has only single chains and spherical micelles with R_h ranging from 14 to 18 nm. The largest micelles form in solutions saturated with water and contain 1.8 water molecules/ethylene oxide repeat unit.[1] We have performed SAXS measurements on cyclopentane solutions of PEO/PS = 65/80 containing spherical micelles and very few single chains. In solutions saturated with water it is difficult to detect any single chains with dynamic light scattering.

A typical SAXS curve for a cyclopentane solution of micelles saturated with water is shown in Figure 6. The lower curve corresponds to the PS = 85 standard which, because of similar degrees of polymerization, represents the scattering expected from the polystyrene blocks isolated in solution. The solid curve is the Debye description of this homopolymer also displayed in the Kratky plot of Figure 3. These curves are most dramatically different at low scattering vectors, with higher

Table IV
Contrasts for PEO/PS = 65/80 Micelles Saturated with Water

		$(\rho_i - \rho_o)/(\rho_i - \rho_o)_{ave}$		
	$(\rho_i - \rho_o)_{ave}$	PS	PEO	H_2O
$(\rho_i^X - \rho_{cp}^X)$,[a] A^{-3}	0.092	0.96	1.26	0.86
$(\rho_i^N - \rho_{ch}^N) \times 10^{-10}$,[b] cm^{-2}	5.94	0.91	1.04	1.26

[a] Electron density difference with cyclopentane as solvent. [b] Scattering length density difference with deuterated cyclohexane as solvent.

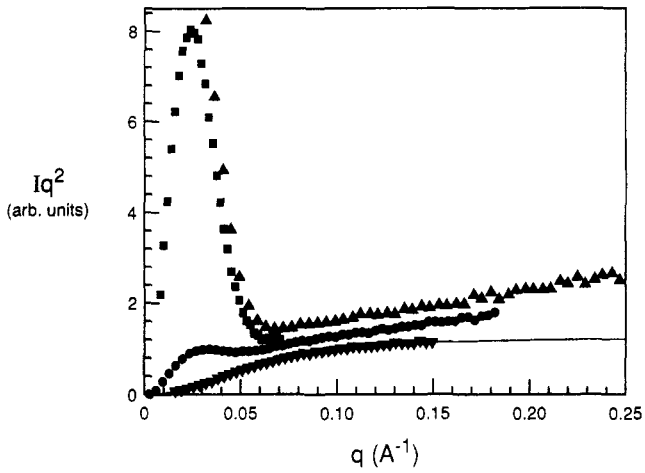

Figure 7. Kratky plots of the data presented in Figure 6. The scattering profiles for the micellar solutions decay as $\sim q^{-1.5}$ at large scattering vectors.

intensities from the micelles due to their larger size. Significant deviations appear again at large scattering vectors that probe the structural details of the micelles and single chains. This is supported by small-angle neutron scattering of PEO/PS = 65/80 micelles saturated with water in deuterated cyclohexane.

Since the Θ temperature for hydrogenated polystyrene in deuterated cyclohexane is 39 °C,[25] we also expect near-Θ conditions for the blocks in the coronae of these micelles observed at 40 °C. Both saturated micelles at 23 °C in cyclopentane and 40 °C in deuterated cyclohexane exhibit a hydrodynamic radius of 18 nm. Therefore, SAXS and SANS measurements afford investigation of these micelles with different contrasts (See Table IV). In the neutron scattering experiments both the water and poly(ethylene oxide) provide more contrast with the solvent than polystyrene, yielding a signal more strongly affected by the micelle core. Since water and PEO have the lowest and highest electron density contrast, respectively, the combination of these two in the micelle core brings the core contrast in the SAXS experiments close to the contrast of polystyrene in the corona.

SANS data for saturated PEO/PS = 65/80 micelles are included in Figure 6. Both the SANS and SAXS data display a transition near $q = 0.06$ Å^{-1} and similar behavior at higher scattering vectors. The larger drop in intensity between the low q plateau and the high q tail for the SANS data is due to the higher relative contrast for the micellar cores. The SANS data extending out to $q = 0.3$ Å^{-1} provide a better comparison of scattering between the homopolymer and micelle solutions at large scattering vectors. Kratky representations in Figure 7 clarify this difference. All three solutions exhibit intensities that decay as $\sim q^{-1.5}$ in the vicinity of $q = 0.1$ Å^{-1}. The scattering from the PS = 85 standard approaches the expected decay of q^{-2} at larger q, while scattering from the micellar solutions continues to scale as $\sim q^{-1.5}$ at higher scattering vectors.

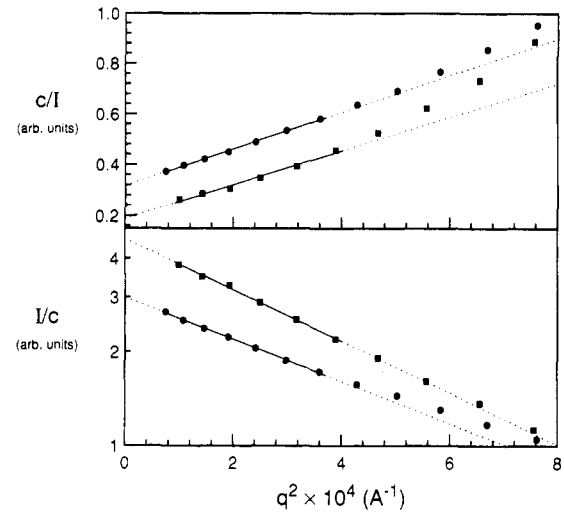

Figure 8. Zimm and Guinier plots above and below, respectively, for PEO/PS = 65/80 micelles saturated with water in (●) cyclopentane (SAXS) and (■) deuterated cyclohexane (SANS).

Thus, the chains in the coronae of PEO/PS = 65/80 micelles do not display the single-chain correlations found in semidilute solutions.

We also note that the log–log representation of the micellar data in Figure 6 displays no indication of a second-order peak from dense micellar cores, as was seen in the study of Plestil and Baldrian.[4] We find indistinguishable scattering behavior at $q > 0.1$ Å^{-1} whether the core has stronger or similar contrast to that from the coronal chains. Even though the PEO/PS = 65/80 micelles contain cores comparable to the coronal size, the scattering in the intermediate region is dominated by contributions from the coronal chains. The effect of enhanced core contrast is evident only at small scattering vectors. Both micellar solutions contain maximums in the Kratky plots at $q \approx 0.03$ Å^{-1}, a more pronounced feature in the SANS data where the dense structure of the core is more strongly weighted. Richter et al. also find a more dramatic peak in SANS Kratky plots of diblock copolymer stars with stronger core contrast.[17] A potential onset of this maximum is visible in the Kratky plot for PEO/PS = 170/1730 micelles saturated with water in Figure 4.

We have used both Guinier and Zimm analyses to measure the micelle radius of gyration; Figure 8 includes SANS and SAXS data for PEO/PS = 65/80 micelles saturated with water. It is noteworthy that the Guinier approximation better represents the SANS data with the stronger contribution from the micellar cores; this is the better method for analyzing scattering from dense globular structures.[29] We find an R_g of 7.6 nm from a Guinier plot of the SANS data. As we described in our analysis of homopolymer solutions, averaging the values from Guinier and Zimm plots, 6.8 and 8.3 nm, respectively, yielding an average R_g of 7.5 nm, appears better suited for describing the SAXS data. Since the difference in contrast between any of the components is smaller than the contrast between the overall micelle and the solvent in the SAXS and SANS experiments, we expect that the *apparent* values we measure are close to the true values of R_g and are not complicated by polydispersity issues.[45]

We can compare our measured R_g with the Gaussian star model of Benoit[46] which predicts the peak in the Kratky plot should occur near $qR_g \approx 1$.[17] This suggests a PEO/PS = 65/80 micelle R_g on the order of 3.5 nm. The inadequacy of the Gaussian model for describing micelles of tightly packed symmetric block copolymer is not

unexpected since it neglects excluded-volume interactions between different chains in the starlike structure. In the other extreme, the portrayal of the micelle corona as a shell of rods extending from a hard core[47] yields an unrealistically large R_g on the order of 21 nm.

The starlike micelle model accounts for screening effects from other chains and should provide an improved description of these micelles. In the SANS experiment, we measure a molecular weight corresponding to 40 chains for PS/PEO = 65/80 micelles saturated with water in deuterated cyclohexane. Using this aggregation number, the starlike model predicts radii of gyration of 6.23 and 6.15 nm for the SAXS and SANS contrasts, respectively; the difference in contrast should have little effect on the measured R_g. The model also predicts an overall micelle radius, R_m, of 9.9 nm, much smaller than the micelle hydrodynamic radius of 18 nm in both the cyclopentane and deuterated cyclohexane solutions. Although the measured R_g from the SAXS and SANS experiments are barely distinguishable from one another, the starlike micelle model does not adequately describe the micelles of the small symmetric copolymer.

A closer look at the proposed micelle structure suggests the origin of the starlike model failure. In the micelle corona the concentration of polystyrene decays with radial distance in a self-similar manner while the blob size corresponding to the local concentration increases continuously. At the surface of the core and at the outer micelle radius we find blob sizes of 2.6 and 6.3 nm, respectively. Hence, one would expect only 3–17 statistical units in the blobs of the PEO/PS = 65/80 micelle coronae. Note that, with five polystyrene repeat units in a statistical unit, each polystyrene block contains only 16 statistical units. Data for the PS = 85 standard discussed earlier illustrate that the isolated blocks are near the limit of molecular weights following Gaussian statistics. When the blocks are constrained to the micelle coronae, the blob sizes are too small to expect single-chain scaling behavior.

In light of these observations, consider again the scattering observed at large scattering vectors. There is a natural tendency for chains in a starlike structure to extend in the radial direction, owing to the lower concentration at the outer edges. The deformation becomes more pronounced with increasing number of arms. In the extreme case found in the PEO/PS = 65/80 micelles, the space between chains is not large enough for the relatively stiff polystyrene chains to undergo a random walk on a local scale. The high-concentration environment with a concentration gradient in the radial direction leads to highly extended chain configurations. The high q decay as $\sim q^{-1.5}$ for the PEO/PS = 65/80 micelles is between the behavior in the intermediate region for random coils, $I \propto q^{-2}$, and scattering of rods, $I \propto q^{-1}$. We find a superposition of scattering at high q from polystyrene in different environments since the concentration is not constant in the micelle corona. The constraints are most severe near the core where the chains are crowded, leading to trajectories persisting more strongly away from the micelle core than in a random walk.

Richter et al. find complementary observations in SANS measurements of 12-arm star polymers synthesized from hydrogenated/deuterated diblock copolymers.[17] Stars with the inner core labeled display perturbed chain configurations similar to the PEO/PS = 65/80 micelles, with a smaller exponent at high q than found in semidilute solutions. On the other hand, when the star molecules are fully labeled, the outer edges of the star dominate and the expected scaling behavior is observed. Unrealistically small blob sizes are also predicted near the core of the PEO/PS = 170/1730 micelles, as illustrated by the schematic diagrams of Figure 9 drawn to scale. Blob sizes near the core are roughly the same size in both micelles saturated with water since $\xi(R_c)$ depends on the micelle aggregation number and the core radius; the PEO/PS = 170/1730 micelles have twice as many chains while the core radius is approximately $\sqrt{2}$ times larger than the PEO/PS = 65/80 micelles. It is significant, however, that only 3% of the polystyrene in the PEO/PS = 170/1730 micelles is in blobs containing less than 10 statistical units. The scattering at high q is dominated by the large blobs at the outer edges of the coronae that contain on the order of 100 statistical units. We expect that, if we could measure only the scattering contribution from the polystyrene near the PEO/PS = 170/1730 micelle cores, we would find scattering from stretched coronal chains similar to that found in the PEO/PS = 65/80 micelles. Since the full PEO/PS = 170/1730 micelle results agree well with model predictions, it is clear that the starlike micelle model is best suited for describing concentration profiles in micelles with moderate aggregation numbers and long coronal blocks.

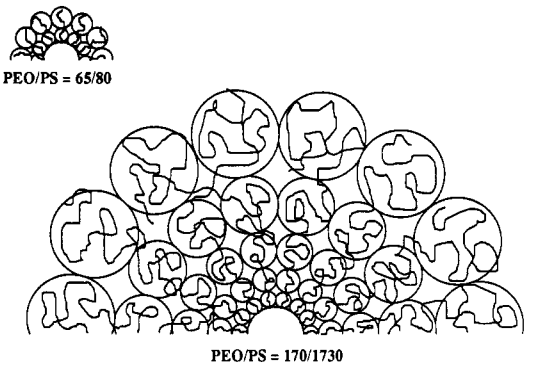

Figure 9. Starlike model predictions of micelle structure drawn to scale. PEO/PS = 65/80 and PEO/PS = 170/1730 micelles saturated with water have aggregation numbers of 40 and 77, core radii of 4.2 and 6.4 nm, and outer micelle radii of 9.9 and 49.7 nm, respectively. Both micelles have blob diameters of 3 nm near the micelle cores.

Conclusions

Interpreting our experimental results in the context of the starlike micelle model, we can characterize micelle structure with three regimes. Coronal chains are least perturbed in micelles with relatively few chains and large soluble blocks. Here large portions of the chains appear as nonoverlapping coils. In the second regime, the configurations of coronal chains can be described by strings of blobs in micelles containing enough chains to form a semidilute solution throughout the micelle corona. Measurements of these micelles coincide with model predictions on both large and small length scales, including previous measurements[2] of micelle radius of gyration and hydrodynamic size (overall size), as well as characterization of the micelle coronae in terms of an average blob size or correlation length. The third regime is characterized by high concentrations in the micelle corona, leading to nonrandom walks away from the micelle core. We find evidence in the intermediate scattering region of severely stretched coronal chains in micelles of short block copolymers.

Acknowledgment. This work has been partially supported by the Center for Materials Research at Stanford University under the NSF–MRL program, the du

Pont Marshall Laboratory, and the Exxon Educational Foundation. The SAXS results presented here were collected at the National Synchrotron Light Source, Brookhaven National Laboratory, which is supported by the U.S. Department of Energy, Division of Materials Sciences and Division of Chemical Sciences (DOE Contract No. DE-AC02-76CH00016), and the Office of Health and Environmental Research (DOE proposals KP04-01 and KP04-B043). Preliminary SAXS work done at SSRL is funded by the DOE under Contract No. DE-AC03-82ER-13000, Office of Basic Energy Sciences, Division of Chemical Sciences, and the NIH, Biotechnology Resource Program Division of Research Sources. Travel grants to NSLS were provided by NSLS and SSRL. K.A.C. appreciates support from the Eastman Kodak Co. and AT&T Bell Laboratories.

We thank Jennifer Raeder for her help in these experiments. We gratefully acknowledge useful discussions with Tom Russell, Soichi Wakatsuki, Bela Farago, and John Huang and technical support from Paul Levin. In addition, we appreciate contributions to the scattering team effort from Frans Leermakers, Lena Vagberg, Pat Dooley, Mark Tracy, and Mark Fair.

References and Notes

(1) Cogan, K. A.; Gast, A. P. *Macromolecules* **1990**, *23*, 745.
(2) Vagberg, L. J. M.; Cogan, K. A.; Gast, A. P. *Macromolecules* **1991**, *24*, 1670.
(3) Milner, S. T. *Science* **1991**, *251*, 905.
(4) Plestil, J.; Baldrian, J. *Makromol. Chem.* **1975**, *176*, 1009.
(5) Noolandi, J.; Hong, K. M. *Macromolecules* **1983**, *16*, 1443.
(6) Leibler, L.; Orland, H.; Wheeler, J. C. *J. Chem. Phys.* **1983**, *79*, 3550.
(7) Munch, M. R.; Gast, A. P. *Macromolecules* **1988**, *21*, 1360.
(8) Nagarajan, R.; Ganesh, K. *J. Chem. Phys.* **1989**, *90*, 5843.
(9) Balsara, N. P.; Tirrell, M.; Lodge, T. P. *Macromolecules* **1991**, *24*, 1975.
(10) Daoud, M.; Cotton, J. P. *J. Phys. (Paris)* **1982**, *43*, 531.
(11) Grest, G. S.; Kremer, K.; Witten, T. A. *Macromolecules* **1987**, *20*, 1376.
(12) Halperin, A. *Macromolecules* **1987**, *20*, 2943.
(13) Batoulis, J.; Kremer, K. *Europhys. Lett.* **1988**, *7*, 683.
(14) Batoulis, J.; Kremer, K. *Macromolecules* **1989**, *22*, 4277.
(15) Huber, K.; Burchard, W.; Fetters, L. J. *Macromolecules* **1984**, *17*, 541.
(16) Bauer, B. J.; Fetters, L. J.; Graessley, W. W.; Hadjichristidis, N.; Quack, G. F. *Macromolecules* **1989**, *22*, 2337.
(17) Richter, D.; Farago, B.; Fetters, L. J.; Huang, J. S.; Ewen, B. *Macromolecules* **1990**, *23*, 1845.
(18) Gast, A. P. Block Copolymers at Interfaces. In *Scientific Methods for the Study of Polymer Colloids and Their Applications*; Ottewill, R. H., Ed.; NATO Advanced Study Institute Series C; Kluwer Academic: Dordrecht, The Netherlands, 1990; p 311.
(19) Dozier, W. D.; Huang, J. S.; Fetters, L. J. *Macromolecules* **1991**, *24*, 2810.
(20) Candau, F.; Guenet, J.-M.; Boutillier, J.; Picot, C. *Polymer* **1979**, *20*, 1227.
(21) Marie, P.; Duplessix, R.; Gallot, Y.; Picot, C. *Macromolecules* **1979**, *12*, 1180.
(22) Brandrup, J., Immergut, E. H., Eds. *Polymer Handbook*, 3rd ed.; Wiley: New York, 1989.
(23) Johnson, B. L.; Smith, J. Refractive Indices and Densities of Some Common Polymer Solvents. In *Light Scattering from Polymer Solutions*; Huglin, M. B., Ed.; Academic Press: London, 1972; p 30.
(24) Russell, T. P.; Lin, J. S.; Spooner, S.; Wignall, G. D. *J. Appl. Crystallogr.* **1988**, *21*, 629.
(25) Strazielle, C.; Benoit, H. *Macromolecules* **1975**, *8*, 203.
(26) Richards, R. W. Molecular Dimensions of Amorphous Polymers by Neutron Scattering. In *Developments in Polymer Characterization*; Dawkin, J. V., Ed.; Applied Science Publishers Ltd.: London, 1978; p 120.
(27) Provencher, S. W.; Hendrix, J.; De Maeyer, L.; Paulussen, N. *J. Chem. Phys.* **1978**, *69*, 4273.
(28) Kratky, O. Natural High Polymers in the Dissolved and Solid State. In *Small Angle X-ray Scattering*; Glatter, O.; Kratky, O., Eds.; Academic Press: London, 1982; p 361.
(29) Kirste, R. G.; Oberthur, R. C. Synthetic Polymers in Solution. In *Small Angle X-ray Scattering*; Glatter, O.; Kratky, O., Eds.; Academic Press: London, 1982; p 387.
(30) Ullman, R. *J. Polym. Sci., Polym. Phys. Ed.* **1985**, *23*, 1477.
(31) Flory, P. J. *Principles of Polymer Chemistry*; Cornell University Press: Ithaca, NY, 1953; p 412.
(32) Berry, G. C. *J. Chem. Phys.* **1966**, *44*, 4550.
(33) Ballard, D. G. H.; Rayner, M. G.; Schelten, J. *Polymer* **1976**, *17*, 349.
(34) Debye, P. *J. Phys. Colloid Chem.* **1947**, *51*, 18.
(35) Kratky, O. *Pure Appl. Chem.* **1966**, *12*, 483.
(36) Yoon, D. Y.; Flory, P. J. *Macromolecules* **1976**, *9*, 294.
(37) de Gennes, P.-G. *Scaling Concepts in Polymer Physics*; Cornell University Press: Ithaca, NY, 1979.
(38) Richter, D.; Stuhn, B.; Ewen, B.; Nerger, D. *Phys. Rev. Lett.* **1987**, *58*, 2462.
(39) Daoud, M.; Cotton, J. P.; Farnoux, B.; Jannink, G.; Sarma, G.; Benoit, H.; Duplessix, R.; Picot, C.; de Gennes, P.-G. *Macromolecules* **1975**, *8*, 804.
(40) King, J. S.; Boyer, W.; Wignall, G. D.; Ullman, R. *Macromolecules* **1985**, *18*, 709.
(41) Brown, W.; Mortensen, K. *Macromolecules* **1988**, *21*, 420.
(42) Edwards, S. F. *Proc. Phys. Soc.* **1966**, *88*, 265.
(43) Berne, B. J.; Pecora, R. *Dynamic Light Scattering*; Wiley: New York, 1976; p 174.
(44) Lantman, C. W.; MacKnight, W. J.; Tassin, J. F.; Monnerie, L.; Fetters, L. J. *Macromolecules* **1990**, *23*, 836.
(45) Burchard, W.; Kajiwara, K.; Nerger, D.; Stockmayer, W. H. *Macromolecules* **1984**, *17*, 222.
(46) Benoit, H. *J. Polym. Sci.* **1953**, *11*, 507.
(47) Hirata, M.; Tsunashima, Y. *Macromolecules* **1989**, *22*, 249.
(48) Higgins, J. S.; Maconnachie, A. Neutron Scattering from Macromolecules in Solution. In *Polymers in Solution*; Forsman, W. C., Ed.; Plenum Press: New York, 1986; p 183.

Registry No. PEO/PS (block copolymer), 107311-90-0.